

# Long-Time Coherence in Echo Spectroscopy with $\pi/2-\pi-\pi/2$ Pulse Sequence

Arseni Goussev

*School of Mathematics, University of Bristol, University Walk, Bristol BS8 1TW, UK*

Philippe Jacquod

*Physics Department, University of Arizona, 1118 E. 4<sup>th</sup> Street, Tucson, AZ 85721, USA*

Motivated by atom optics experiments, we investigate a new class of fidelity functions describing the reconstruction of quantum states by time-reversal operations as  $M_{\text{Da}}(t) = |\langle \psi | e^{iH_2 t/2} e^{iH_1 t/2} e^{-iH_2 t/2} e^{-iH_1 t/2} | \psi \rangle|^2$ . We show that the decay of  $M_{\text{Da}}$  is quartic in time at short times, and that it freezes well above the ergodic value at long times, when  $H_2 - H_1$  is not too large. The long-time saturation value of  $M_{\text{Da}}$  contains easily extractable information on the strength of decoherence in these systems.

PACS numbers: 05.45.Mt, 03.65.Yz

## I. INTRODUCTION

When subjected to external noisy fields, quantum mechanical wavefunctions lose memory of their phase. As a fundamentally important consequence of this *decoherence* process, pairs of partially scattered waves no longer interfere, and the dynamics follows the Liouville time-evolution of classical densities [1]. A somehow similar situation occurs when one time-evolves an initial superposition  $\phi = \sum_{\alpha} c_{\alpha} \psi_{\alpha}$  of many eigenmodes  $\psi_{\alpha}$  of the Hamiltonian  $H_1$  governing the time evolution, with incommensurate eigenfrequencies  $\epsilon_{\alpha}$ . In this case, for each pair of components  $(\alpha, \beta)$ , the relative phase  $(\epsilon_{\alpha} - \epsilon_{\beta})t$  becomes pseudo-random, which washes out partial wave interferences. This *dephasing* process, however, differs from decoherence in a fundamental way that it can in principle be undone by an appropriate time-inversion. As a matter of fact, echo experiments are able to reverse the sign of the Hamiltonian,  $H_1 \rightarrow -H_1$ , by means of effective changes of coordinate axes induced by electromagnetic pulses [2]. When this operation is performed after an evolution time  $t$ , one expects the initial wavefunction to be reconstructed at  $2t$ , regardless of its spread over eigenmodes. Imperfections in the pulse sequence or unavoidable couplings to external uncontrolled degrees of freedom result instead in an imperfect time-inversion,  $H_1 \rightarrow -H_2 = -H_1 - \Sigma$ , and therefore the Loschmidt echo [15–18, 20] (we set  $\hbar \equiv 1$ )

$$M_{\text{L}}(t) = |m_{\text{L}}(t)|^2, \quad \text{with} \quad (1a)$$

$$m_{\text{L}}(t) = \langle \psi | e^{iH_2 t} e^{-iH_1 t} | \psi \rangle, \quad (1b)$$

gives a better description of the fidelity with which the experiment reconstructs the initial state. Echo experiments in nuclear magnetic resonance [2, 3], quantum optics [4], atomic [5–7], condensed matter [8], microwave cavities [9], and elastodynamics [10] have demonstrated that  $M_{\text{L}}(t)$  remains sizable for times significantly longer than the dephasing time. The decay of  $M_{\text{L}}(t)$  allows one to extract information on irreversible decoherence processes induced by  $\Sigma$ .

In experiments with cold atoms the Loschmidt echo,  $M_{\text{L}}$ , can be extracted from interference fringes of Ramsey spectroscopy [11]. There, an effectively two-level atom is initially prepared in a state  $|1\rangle \otimes |\psi\rangle$ , where  $|1\rangle$  and  $|2\rangle$  denote the two internal atomic states, and  $|\psi\rangle$  stands for the spatial component of the initial state. First, the atom is irradiated with a microwave frequency field with energy chosen to change the atomic state into an equiprobable superposition of  $|1\rangle \otimes |\psi\rangle$  and  $|2\rangle \otimes |\psi\rangle$ . Such a field is referred to as a  $\pi/2$  pulse. The atom is then let to evolve in an optical trap for a time  $t$  during which the  $|1\rangle$ -component of the state evolves under a spatial Hamiltonian  $H_1$ , while the  $|2\rangle$ -component under  $H_2$ . After that another  $\pi/2$  pulse is applied to the atom and the probability  $P_2$  for the atom to be found in the internal state  $|2\rangle$  is measured. It turns out that this probability is essentially determined by the Loschmidt echo amplitude,  $m_{\text{L}}$ . In practice however one works not with a pure initial state  $|\psi\rangle$ , but with a thermal mixture of initial states. The echo amplitude  $m_{\text{L}}$  from each of these states contributes to  $P_2$  with a different, effectively random phase, which in turn reduces the fringe contrast in a Ramsey experiment. As a result, the  $\pi/2-\pi-\pi/2$  pulse sequence proves inefficient in measuring the Loschmidt echo for large ensembles of thermally populated states.

In order to overcome this difficulty Davidson and collaborators implemented a novel pulse sequence in their echo spectroscopy experiments [6, 7]

$$M_{\text{Da}}(t) = |m_{\text{Da}}(t)|^2, \quad \text{with} \quad (2a)$$

$$m_{\text{Da}}(t) = \langle \psi | e^{iH_2 t/2} e^{iH_1 t/2} e^{-iH_2 t/2} e^{-iH_1 t/2} | \psi \rangle. \quad (2b)$$

The corresponding pulse sequence consisted of three short pulses,  $\pi/2-\pi-\pi/2$ , separated by two time intervals of equal duration  $t/2$ , after which  $P_2$  was measured. The  $\pi$  pulse swaps the population of the internal states  $|1\rangle$  and  $|2\rangle$ . The probability  $P_2$  is then determined by the amplitude  $m_{\text{Da}}$ , and each individual state of the thermal ensemble contributes to  $P_2$  with the same phase. Thus, the  $\pi/2-\pi-\pi/2$  pulse sequence allows one to measure the echo in Eq. (2) even for ensembles of more than  $10^6$  of thermally populated states, as in the experiments

of Refs. [6, 7].

It is clear from the definitions given by Eqs. (1) and (2) that mathematically  $M_{\text{Da}}$  is not the same quantity as the Loschmidt echo  $M_{\text{L}}$ . Even though some significant differences between  $M_{\text{Da}}$  and  $M_{\text{L}}$  have been previously envisaged in the literature they have never been systematically studied. It is the purpose of this article to fill in this gap by comparing the two quantities both analytically and numerically. Below, we show that  $M_{\text{Da}}$  differs from the Loschmidt echo  $M_{\text{L}}$  in the two important respects that (i) its short-time decay is quartic and not quadratic in time, and (ii) for not too strong perturbation  $\Sigma = H_2 - H_1$ ,  $M_{\text{Da}}$  saturates at a perturbation-dependent value, well above the ergodic saturation of  $M_{\text{L}}(\infty) \sim N^{-1}$  at the inverse Hilbert space size. Fidelity freezes have been reported for Loschmidt echoes with off-diagonal perturbations with a zero time average [12], phase-space displacement perturbations [13], and more recently for initially pure states coupled to complex environments [14], however the freeze we report here has a different physical origin. We note in particular that it persists for  $t \rightarrow \infty$ . The long-time saturation of  $M_{\text{Da}}$  allows to extract the strength of the fields in  $\Sigma$  more easily than by fitting decay curves of conventional echoes, over not precisely defined time intervals. Moreover, the absence of decay arising from  $\Sigma$  in this pulse sequence makes it straightforward to extract decoherence rates because, assuming that the pulse sequence is perfect, any decay in experimentally obtained data for  $M_{\text{Da}}(t)$  would come exclusively from the coupling of the system to external degrees of freedom, not included in our theory. Given the superb experimental control that modern echo experiments have on their pulse sequence, this novel echo spectroscopy has therefore the potential to deliver precious, previously unattainable information on the dominant sources of decoherence in trapped cold atomic gases.

## II. SHORT-TIME DECAY

There has been a large number of analytical and numerical investigations of the Loschmidt echo and some of its offsprings [15, 16]. Most, if not all approaches assume a small perturbation, i.e.  $|\Sigma| \ll |H_{1,2}|$  for an appropriate operator norm. As but one consequence, the largest energy scale is the energy bandwidth  $B$ , which to leading order is the same for  $H_1$  and  $H_2$ . For short times,  $t \ll B^{-1}$ ,  $M_{\text{L}}(t)$  is easily calculated by expanding the propagators in Eqs. (1), and keeping the leading order contributions. One obtains

$$M_{\text{L}}(t) \simeq 1 - (\sigma_{\text{L}}t)^2, \quad (3)$$

where

$$\sigma_{\text{L}}^2 = \langle \psi | \Sigma_{\text{L}}^2 | \psi \rangle - \langle \psi | \Sigma_{\text{L}} | \psi \rangle^2, \quad \Sigma_{\text{L}} = H_1 - H_2. \quad (4)$$

Thus, the short-time decay of the Loschmidt echo is *quadratic* [17, 18], with a rate given by the dispersion

$\sigma_{\text{L}}$  of the perturbation operator  $\Sigma_{\text{L}}$  evaluated over the initial state.

The same procedure can be applied to  $M_{\text{Da}}$ , where it however gives

$$M_{\text{Da}}(t) \simeq 1 - (\sigma_{\text{Da}}t)^4, \quad (5)$$

with the decay rate  $\sigma_{\text{Da}}$  given by

$$\sigma_{\text{Da}}^4 = \langle \psi | \Sigma_{\text{Da}}^2 | \psi \rangle - \langle \psi | \Sigma_{\text{Da}} | \psi \rangle^2, \quad \Sigma_{\text{Da}} = \frac{i}{4} [H_1, H_2]. \quad (6)$$

Two things are remarkable here. First, the short-time decay of  $M_{\text{Da}}$  is *quartic* in  $t$ , and thus slower than the decay of  $M_{\text{L}}$ . Second, its rate is determined by the *commutator* of the unperturbed and perturbed Hamiltonians.

## III. LONG-TIME SATURATION

The analysis of the long-time behavior of  $M_{\text{L}}$  and  $M_{\text{Da}}$  starts by diagonalizing the unperturbed and perturbed Hamiltonian operators,  $H_1 = \sum_u E_u |u\rangle\langle u|$  and  $H_2 = \sum_v E_v |v\rangle\langle v|$ , and expanding the initial state in the basis of the unperturbed Hamiltonian,  $|\psi\rangle = \sum_u c_u |u\rangle$  [16]. The resulting expression for the echo is then averaged over time to yield the mean saturation value. In the case of the Loschmidt echo the time-averaged saturation is given by

$$M_{\text{L},\infty} = \sum_{u,u',u'',v} c_u^* c_{u''} |c_{u'}|^2 \langle u|v\rangle\langle v|u'\rangle\langle u'|v\rangle\langle v|u''\rangle. \quad (7)$$

The next step is to average this expression over a random ensemble of coefficient  $c_u$  for the initial state, such that  $\overline{c_u^* c_{u'}} = N^{-1} \delta_{u,u'}$ . (Hereinafter, an overline denotes the averaging over an ensemble of random initial states.) Here  $N$  is the effective size of the Hilbert space (the number of eigenstates of  $H_{1,2}$  comprising the initial state). To leading order in  $1/N$ , one uses  $\overline{c_u^* c_{u''} |c_{u'}|^2} = \overline{c_u^* c_{u''}} \cdot \overline{|c_{u'}|^2} = N^{-2} \delta_{u,u''}$  to obtain the ergodic saturation value

$$\overline{M_{\text{L},\infty}} = \frac{1}{N}. \quad (8)$$

Using the same procedure, one can calculate the long-time saturation value of  $M_{\text{Da}}$ . At the level of the echo amplitude  $m_{\text{Da}}$ , one gets

$$\overline{m_{\text{Da},\infty}} = \sum_{u,u',v} \overline{c_u^* c_{u'}} \langle u|v\rangle\langle v|u'\rangle\langle u'|v\rangle\langle v|u'\rangle \quad (9a)$$

$$= \frac{1}{N} \sum_{u,v} |\langle u|v\rangle|^4. \quad (9b)$$

One then uses an approximation  $|\langle u|v\rangle|^4 \simeq \overline{|\langle u|v\rangle|^2}^2$  with  $\overline{|\langle u|v\rangle|^2} = \rho(E_u - E_v)$  a function of only the energy difference between the two states. Replacing one of the sums

in Eq. (9) by an integral over the energy difference between the two states scaled by the mean level spacing  $\Delta = B/N$ , we can write

$$\overline{m_{\text{Da},\infty}} \simeq \int \frac{dE}{\Delta} \rho^2(E). \quad (10)$$

This expression relates the long-time saturation of  $M_{\text{Da}}$  to the energy spreading of eigenfunctions of  $H_1$  over those of  $H_2$  as measured by  $\rho(E)$ . It is known for a large variety of quantum chaotic systems that, in the regime  $\Delta \ll \Gamma/\Delta \ll B$ , this spreading has a Lorentzian shape

$$\rho(E_u - E_v) \simeq \frac{\Delta}{\pi} \frac{\Gamma/2}{(E_u - E_v)^2 + (\Gamma/2)^2}, \quad (11)$$

with a spreading width given by the golden rule,  $\Gamma \simeq \sigma_L^2/\Delta$  [19], see Eq. (4) for the definition of  $\sigma_L^2$ . We thus obtain

$$\overline{m_{\text{Da},\infty}} \simeq \frac{\Delta}{\pi\Gamma}. \quad (12)$$

Eqs. (11) and (12) predict an average saturation value  $\overline{M_{\text{Da},\infty}}$  above the ergodic saturation for  $N < (B/\pi\Gamma)^2$ . The width  $\Gamma$  of the Lorentzian (11) increases with  $|\Sigma|$ , and the ergodic saturation, Eq.(8), is recovered when  $\Gamma > B/\pi N^{1/2}$ , thus

$$\overline{M_{\text{Da},\infty}} \simeq \max \left[ \left( \frac{\Delta}{\pi\Gamma} \right)^2, \frac{1}{N} \right]. \quad (13)$$

We note that the Lorentzian spreading of Eq. (11) is replaced by more complicated, system-dependent spiked structures in dynamical systems with mixed or regular dynamics, for which it is accordingly impossible to draw general conclusions. We stress, however, that Eq. (10) remains valid even in that case.

Eq. (13) is the main result of this paper. This new long-time fidelity saturation originates from the specific sequence of time-evolutions in  $M_{\text{Da}}$ , giving the long-time behavior of the latter as an energy integral over the *squared* average overlap  $|\langle u|v\rangle|^4$  of eigenstates  $|u\rangle$  of  $H_1$  over the eigenstates  $|v\rangle$  of  $H_2$ . For completeness we next comment on the intermediate regime, between the short-time quartic decay and the long-time saturation.

#### IV. INTERMEDIATE ASYMPTOTIC DECAY

We briefly sketch a semiclassical analysis of  $M_{\text{Da}}$  in the intermediate regime between the short-time decay and the long-time saturation. We follow the lines of Ref. [20] to show that  $M_{\text{Da}}$  and  $M_L$  have the same behavior in that regime.

In the semiclassical approximation the time evolution of  $|\psi\rangle$  under  $H_j$ ,  $j = 1, 2$ , is given by

$$\langle \mathbf{r} | e^{-iH_j t} | \psi \rangle = \int d\mathbf{r}' \sum_{\gamma(\mathbf{r}' \rightarrow \mathbf{r}, t)} D_{j,\gamma} e^{iS_{j,\gamma}} \langle \mathbf{r}' | \psi \rangle. \quad (14)$$

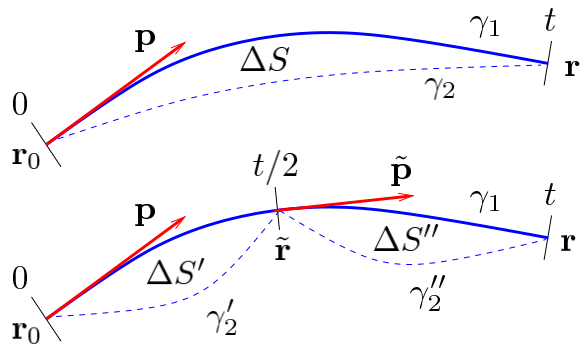


Figure 1: (Color online) Trajectories of the unperturbed ( $\gamma_1$ ) and perturbed ( $\gamma_2$ ,  $\gamma'_2$ , and  $\gamma''_2$ ) systems together with the associated action differences ( $\Delta S$ ,  $\Delta S'$ , and  $\Delta S''$ ).

Here, the sum goes over all classical paths  $\gamma$  connecting  $\mathbf{r}'$  and  $\mathbf{r}$  in time  $t$ ,  $S_{j,\gamma} = S_{j,\gamma}(\mathbf{r}, \mathbf{r}', t)$  is the action along  $\gamma$ ,  $D_{j,\gamma} = (2\pi i)^{-d/2} |\det(\partial^2 S_{j,\gamma} / \partial \mathbf{r} \partial \mathbf{r}')|^{1/2} e^{-i\pi\nu_{j,\gamma}/2}$  with Morse index  $\nu_{j,\gamma}$  counting the number of conjugate points on  $\gamma$ , and  $d$  is the dimensionality of the system [21]. The semiclassical Loschmidt echo amplitude is obtained by inserting Eq. (14) in Eq. (1b). The resulting expression contains three spatial integrals over  $\mathbf{r}$ ,  $\mathbf{r}'$ , and  $\mathbf{r}''$  with a double sum over trajectories  $\gamma_1(\mathbf{r}' \rightarrow \mathbf{r}, t)$  and  $\gamma_2(\mathbf{r}'' \rightarrow \mathbf{r}, t)$  corresponding to the Hamiltonians  $H_1$  and  $H_2$  respectively. The standard analysis of this expression involves three steps [20]: (i) One assumes that  $\langle \mathbf{r} | \psi \rangle$  is localized about a point  $\mathbf{r}_0$  and evaluates the integrals over  $\mathbf{r}'$  and  $\mathbf{r}''$  by stationary phase approximations. This reduces the set of paths  $\gamma_1$  and  $\gamma_2$  to those starting at  $\mathbf{r}_0$ , see Fig. 1. (ii) Noting that the double sum over trajectories contains rapidly oscillating phase factors  $\exp[i(S_{1,\gamma_1} - S_{2,\gamma_2})]$ , so that only pairs of correlated paths  $\gamma_1$  and  $\gamma_2$  contribute to  $m_{\text{Da}}$ , one employs the diagonal approximation ( $\gamma_2 \simeq \gamma_1$ ) to reduce  $m_L$  to a sum over a single path  $\gamma_1$ . Ref. [22], building up on ideas first expressed in Ref. [18], justified this step by the shadowing theorem. (iii) Finally, one uses the fact that  $|D_{1,\gamma_1}|^2$  is the Jacobian of a transformation between final positions  $\mathbf{r}$  and initial momenta  $\mathbf{p}$  on paths  $\gamma_1$ . This allows one to change the integration variable from  $\mathbf{r}$  to  $\mathbf{p}$  to get

$$m_L(t) = (2\pi)^{-d} \int d\mathbf{p} e^{i\Delta S} |\langle \mathbf{p} | \psi \rangle|^2. \quad (15)$$

Here  $\Delta S = \Delta S(\mathbf{r}_0, \mathbf{p}, t) = S_{1,\gamma_1} - S_{2,\gamma_2}$  is the difference between the action of an unperturbed trajectory  $\gamma_1$  leaving the point  $\mathbf{r}_0$  with a momentum  $\mathbf{p}$  and traveling for time  $t$  and the action of the corresponding perturbed trajectory  $\gamma_2 \simeq \gamma_1$ . Following the same procedure one finds

$$m_{\text{Da}}(t) = (2\pi)^{-d} \int d\mathbf{p} e^{i(\Delta S' - \Delta S'')} |\langle \mathbf{p} | \psi \rangle|^2, \quad (16)$$

where  $\Delta S' = \Delta S(\mathbf{r}_0, \mathbf{p}, t/2)$  and  $\Delta S'' = \Delta S(\tilde{\mathbf{r}}, \tilde{\mathbf{p}}, t/2)$  with  $(\tilde{\mathbf{r}}, \tilde{\mathbf{p}})$  being the phase space point on  $\gamma_1$  at time  $t/2$ , see Fig. 1. In other words,  $\Delta S'$  ( $\Delta S''$ ) is the action

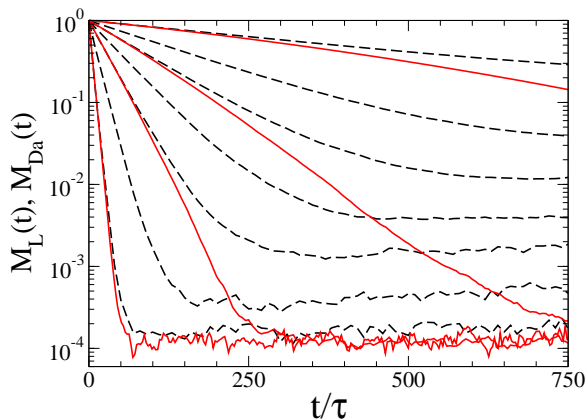


Figure 2: (Color online) Average echo decay for the kicked rotator model with  $K_1 = 57$ ,  $N = 8192$ , and  $K_2 - K_1 = 5 \cdot 10^{-5}$ ,  $1.2 \cdot 10^{-4}$ ,  $2.1 \cdot 10^{-4}$  and  $5 \cdot 10^{-4}$  ( $M_L$ , red solid lines from top to bottom), and  $K_2 - K_1 = 5 \cdot 10^{-5}$ ,  $9 \cdot 10^{-5}$ ,  $1.2 \cdot 10^{-4}$ ,  $1.6 \cdot 10^{-4}$ ,  $2.1 \cdot 10^{-4}$ ,  $3.1 \cdot 10^{-4}$ , and  $5 \cdot 10^{-4}$  ( $M_{Da}$ , black dashed lines, from top to bottom). Curves are averages over 500 initial states.

difference between the first (second) half of the unperturbed trajectory  $\gamma_1$  and the corresponding perturbed trajectory  $\gamma'_2$  ( $\gamma''_2$ ). This is sketched in Fig. 1.

Once averaged over an ensemble of initial states, both  $M_L$  and  $M_{Da}$  satisfy

$$\overline{M_{L,Da}(t)} \simeq \overline{m_{L,Da}(t)}^2 + (2\pi)^{-2d} \int d\mathbf{p} \int_{\Omega_{\mathbf{p}}} d\mathbf{p}' |\langle \mathbf{p} | \psi \rangle|^2 |\langle \mathbf{p}' | \psi \rangle|^2, \quad (17)$$

where the integral over  $\mathbf{p}'$  is restricted to a volume  $\Omega_{\mathbf{p}}$  around  $\mathbf{p}$ , such that two trajectories starting from the same spatial point with momenta  $\mathbf{p}$  and  $\mathbf{p}' \in \Omega_{\mathbf{p}}$  stay “close” in phase space during time  $t$ . The first term in the right-hand side of Eq. (17) is evaluated using the central limit theorem,  $\overline{\exp(i\Delta S)} \simeq \exp(-\overline{\Delta S^2}/2) \simeq e^{-\Gamma t/2}$  and  $\overline{\exp[i(\Delta S' - \Delta S'')]} \simeq \exp[-(\overline{\Delta S'^2} + \overline{\Delta S''^2})/2] \simeq e^{-\Gamma(t/2+t/2)/2} = e^{-\Gamma t/2}$ , where  $\Gamma$  is defined in Eq. (11) as the width of the local density of states. For  $M_{Da}$ , we neglect correlations between  $\Delta S'$  and  $\Delta S''$ , which is justified by the fast decay of correlations along chaotic classical trajectories. The second term in Eq. (17) is determined by the measure of the set  $\Omega_{\mathbf{p}}$  and in chaotic systems decays as  $e^{-\lambda t}$  with  $\lambda$  being the average Lyapunov exponent of the underlying classical system [20]. Therefore, the intermediate time decay of  $M_{Da}$  is the same as that of  $M_L$  [20, 23], i.e.

$$\overline{M_L(t)} \simeq \overline{M_{Da}(t)} \sim e^{-t \min[\Gamma, \lambda]}. \quad (18)$$

This exponential time decay continues until the echo reaches the saturation plateau given by Eq. (13).

Ref. [6] reported some saturation of  $M_{Da}$  for ultracold atoms inside optical traps. However, at this stage, a

direct comparison of these experiments with our theory does not seem feasible, because they explore completely different time regimes. Indeed, the echo spectroscopy experiments of Refs. [6, 7] are concerned with short times corresponding to no more than 3-4 oscillations/bounces of an atom in the trap. In contrast, the semiclassical derivation of the exponential decay, Eq. (18), and the RMT analysis of the fidelity freeze, Eq. (13), are only valid for times much longer than the average free flight time.

## V. NUMERICAL STUDY

We confirm our analytical results with some numerical data. Our simulations are based on the kicked rotator model with dimensionless Hamiltonian

$$H_{1,2} = \frac{\hat{p}^2}{2} + K_{1,2} \cos \hat{x} \sum_n \delta(t - n\tau). \quad (19)$$

For large enough kicking strength,  $K_{1,2}\tau > 7$ , the dynamics is fully chaotic with a Lyapunov exponent  $\lambda = \ln[K_{1,2}\tau/2]$ . We quantize this Hamiltonian on a torus, and accordingly consider discrete values  $p_l = 2\pi l/N$  and  $x_l = 2\pi l/N$ ,  $l = 1, \dots, N$ , giving an effective Planck’s constant  $\hbar_{\text{eff}} = 1/N$ . Both echoes  $M_L(n)$  and  $M_{Da}(n)$  are computed for discrete times  $t = n\tau$ , with the kicking period  $\tau$ , using the unitary Floquet operators  $U_{1,2} = \exp[-i\hat{p}^2/2\hbar_{\text{eff}}] \exp[-iK_{1,2} \cos \hat{x}/\hbar_{\text{eff}}]$  for single-kick time-evolutions. The bandwidth is  $B = 2\pi$  and accordingly  $\Delta = 2\pi/N$ . The eigenstates of  $U_2$  spread over those of  $U_1$  according to Eq. (11) with  $\Gamma \propto (\delta K N)^2$ , with  $\delta K = K_2 - K_1$  [16]. Together with Eq. (13), we thus expect a long-time saturation of  $M_{Da}$  at a value

$$\overline{M_{Da,\infty}} \sim (\delta K^2 N^3)^{-2}, \quad (20)$$

for  $\delta K^4 N^5 < 1$ .

Fig. 2 shows the time decay of the echoes,  $\overline{M_L(t)}$  shown as red curves and  $\overline{M_{Da}(t)}$  as black curves, averaged over an ensemble of randomly chosen initial states. For equal values of the perturbation strength, both  $M_L$  and  $M_{Da}$  display an exponential time decay governed by the same decay rate, providing a clear support for Eq. (18). The Loschmidt echo decay saturates at a value  $\sim N^{-1}$  in agreement with Eq. (8). The freeze of  $M_{Da}$  occurs at a value that decreases with increasing perturbation strength until it reaches ergodic saturation at  $N^{-1}$ . We confirm in Fig. 3 that the numerically observed perturbation-dependent saturation of  $M_{Da}$  follows Eq. (20). Once plotted as a function of  $\delta K N^{3/2}$ , saturation data for  $N \in [256, 8192]$  and  $\delta K \in [4 \cdot 10^{-5}, 0.052]$  nicely fall on top of one another until they deviate because they have different ergodic saturation,  $N^{-1}$ . Moreover, in the regime of validity  $\Delta \ll \delta K \ll B$  of Eq. (11), one has  $M_{Da,\infty} \propto (\delta K N^{3/2})^b$  with an exponent  $b \simeq 3.8$  close to the prediction  $b = 4$  from Eq. (20). We note that

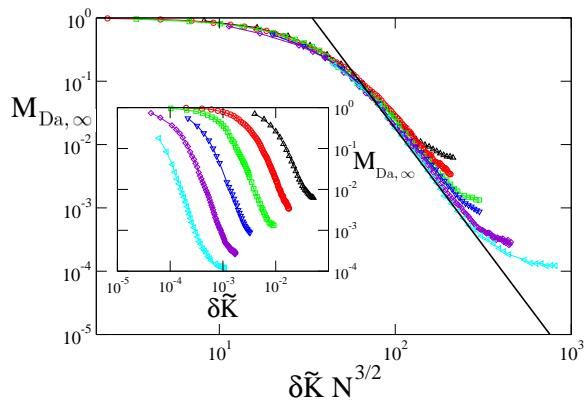


Figure 3: (Color online) Long-time saturation value of  $M_{\text{Da}}$  for  $K_1 = 57$  and  $N = 256$  (black up triangles), 512 (red circles), 1024 (green squares), 2048 (blue down triangles), 4096 (violet diamonds) and 8192 (cyan left triangles). Main panel: rescaled data confirming the analytical prediction of Eq.(20). The straight black line indicates a slope of  $\propto 1/x^{3.8}$ . Inset: raw data as function of the difference of dimensionless kicking strengths  $\delta\tilde{K} = \tilde{K}_2 - \tilde{K}_1$ , with  $\tilde{K}_{1,2} = K_{1,2}/\tau$ .

$b$  is larger for data with larger Hilbert space size  $N$ , where the fitting range is larger – and the fit is accordingly more accurate – because saturation occurs at larger values of  $\delta\tilde{K}N^{3/2}$ . We also checked numerically that the initial decay of  $M_{\text{Da}}$  is quartic and not quadratic in time. Our numerical simulations thus fully confirm the theoretical

predictions derived above.

## VI. CONCLUSIONS

Our analysis of the new fidelity function  $M_{\text{Da}}$  [6, 7] shows that it significantly differs from the Loschmidt echo in two important respects: (i) the short-time decay of  $M_{\text{Da}}$  is quartic (and not quadratic) in time, and is governed by the commutator (and not the difference) of the unperturbed and perturbed Hamiltonians, and (ii) for not too strong Hamiltonian perturbations, the decay of  $M_{\text{Da}}$  freezes at values inversely proportional to the square of the measure  $\Gamma$  of the perturbation, as defined by the width of the local density of states, Eq. (11). This allows to estimate the strength of decoherence processes in systems of cold trapped atoms by fitting the saturation value of  $M_{\text{Da}}$ , which is arguably easier and more precise than fitting decay curves over not precisely defined time intervals. In addition to providing an analytic derivation of this finding, in particular relating the saturation level to the strength of decoherence fields, and to predicting an initial quartic decay of  $M_{\text{Da}}$ , our theory gives an intermediate behavior of  $M_{\text{Da}}$  which follows that of the Loschmidt echo  $M_{\text{L}}$ . We confirmed these analytical findings numerically.

*Acknowledgments.* – A.G. acknowledges the support by EPSRC under Grant No. EP/E024629/1.

- 
- [1] E. Joos, H. D. Zeh, C. Kiefer, D. Giulini, J. Kupsch, I.-O. Stamatescu, *Decoherence and the Appearance of a Classical World in Quantum Theory* (Springer, Berlin 2003).
- [2] E. L. Hahn, Phys. Rev. **80**, 580 (1950).
- [3] A. Z. Zhang, B. H. Meier, and R. R. Ernst, Phys. Rev. Lett. **69**, 2149 (1992).
- [4] N. A. Kurnit, I. D. Abella, and S. R. Hartmann, Phys. Rev. Lett. **13**, 567 (1964).
- [5] F. B. J. Buchkremer, R. Dumke, H. Levens, and W. Ertmer, Phys. Rev. Lett. **85**, 3121 (2000).
- [6] M. F. Andersen, A. Kaplan, and N. Davidson, Phys. Rev. Lett. **90**, 023001 (2003).
- [7] M. F. Andersen, T. Grönzweig, A. Kaplan, and N. Davidson, Phys. Rev. A **69**, 063413 (2004); M. F. Andersen, A. Kaplan, T. Grönzweig, and N. Davidson, Phys. Rev. Lett. **97**, 104102 (2006).
- [8] Y. Nakamura, Yu. A. Pashkin, T. Yamamoto, and J. S. Tsai, Phys. Rev. Lett. **88**, 047901 (2002).
- [9] R. Schäfer, H.-J. Stöckmann, T. Gorin, and T. H. Seligman, Phys. Rev. Lett. **95**, 184102 (2005); R. Schäfer, T. Gorin, T. H. Seligman, and H.-J. Stöckmann, New J. Phys. **7**, 152 (2005).
- [10] T. Gorin, T. H. Seligman, and R. L. Weaver, Phys. Rev. E **73**, 015202(R) (2006); O. I. Lobkis and R. L. Weaver, Phys. Rev. E **78**, 066212 (2008).
- [11] See Refs. [6, 7] for details on experimental techniques of Ramsey and echo spectroscopy.
- [12] T. Prosen and M. Znidaric, New J. Phys. **5**, 109 (2003); Phys. Rev. Lett. **94**, 044101 (2005).
- [13] C. Petitjean, D. V. Bevilacqua, E. J. Heller, and Ph. Jacquod, Phys. Rev. Lett. **98**, 164101 (2007).
- [14] H. Kohler, H.-J. Sommers, S. Åberg, and T. Guhr, Phys. Rev. E **81**, 050103(R) (2010).
- [15] T. Gorin, T. Prosen, T. H. Seligman, and M. Znidaric, Phys. Rep. **435**, 33 (2006).
- [16] Ph. Jacquod and C. Petitjean, Adv. Phys. **58**, 67 (2009).
- [17] A. Peres, Phys. Rev. A **30**, 1610 (1984).
- [18] N. R. Cerruti and S. Tomsovic, Phys. Rev. Lett. **88**, 054103 (2002).
- [19] E. P. Wigner, Ann. Math. **62**, 548 (1955); V. V. Flambaum, A. A. Gribakina, G. F. Gribakin, and M. G. Kozlov, Phys. Rev. A **50**, 267 (1994); Ph. Jacquod and D. L. Shepelyansky, Phys. Rev. Lett. **75**, 3501 (1995); J. L. Gruver, J. Aliaga, H. A. Cerdeira, P. A. Mello, and A. N. Proto, Phys. Rev. E **55**, 6370 (1997).
- [20] R. A. Jalabert and H. M. Pastawski, Phys. Rev. Lett. **86**, 2490 (2001); F. M. Cucchietti, H. M. Pastawski, and R. A. Jalabert, Phys. Rev. B **70**, 035311 (2004).
- [21] M. C. Gutzwiller, *Chaos in Classical and Quantum Mechanics* (Springer, New York, 1990).
- [22] J. Vanicek, Phys. Rev. E **73**, 046204 (2006).
- [23] Ph. Jacquod, P. G. Silvestrov, and C. W. J. Beenakker, Phys. Rev. E **64**, 055203(R) (2001).